# Reactive liquid–liquid extraction of bio-based 3-hydroxypropionic acid using a biocompatible organic phase containing a tertiary amine: A model-based approach to elucidate dominant mechanisms

Pedro Arana-Agudelo, Marwen Moussa, Ioan-Cristian Trelea, Kevin Lachin, Violaine Athès

# *Reactive liquid-liquid extraction of bio-based 3-hydroxypropionic acid using a biocompatible organic phase containing a tertiary amine: a model-based approach to elucidate dominant mechanisms*

Pedro Arana-Agudelo, Marwen Moussa, Ioan-Cristian Trelea, Kevin Lachin, Violaine Athès

Université Paris-Saclay, INRAE, AgroParisTech, UMR SayFood, F-91120, Palaiseau, France

Corresponding author: marwen.moussa@agroparistech.fr

DOI: 10.1016/j.seppur.2022.121184

**Abstract**

This work studies reactive liquid-liquid extraction of 3-hydroxypropionic acid (3-HP) from aqueous solutions using a biocompatible organic phase consisting in N,N-didodecylmethylamine (DDMA) (20% v/v) diluted in 1-dodecanol (40% v/v) and dodecane (40% v/v). The objective was to propose an equilibrium model based on the law of mass action accounting for the main phenomena occurring in the system. A set of equilibrium extraction experiments was performed in the initial acid concentration range 0.0028 – 1 mol $L^{-1}$ in order to determine the extraction yield, equilibrium pH and to collect infrared spectra of the loaded organic phases. FT-IR spectra allowed to identify and elucidate the main mechanisms of acid-amine interaction, which were taken into account in the model. The formation of 1:1 acid-amine stoichiometry complex through ion-pairing was determined as the dominant mechanism in all the concentration range. For initial acid concentrations above 0.11 mol $L^{-1}$, the formation of 2:1 acid-amine complexes through H-bonding of acid molecules with 1:1 complexes was also observed and determined to be almost as important as ion-pair formation at 1 mol $L^{-1}$. The presence of impurities in the organic phase was taken into account by introducing a side reaction essential to represent low extraction yields and high equilibrium pH values observed at low initial acid concentrations ($< 0.02$ mol $L^{-1}$). A global sensitivity analysis of the model's parameters pointed out three concentration regions based on the relative contribution of each phenomenon: (i) for initial acid concentrations below 0.02 mol $L^{-1}$, the main phenomena are 1:1 ion-pair formation and the side reaction; (ii) between 0.02 mol $L^{-1}$ and 0.11 mol $L^{-1}$, mainly 1:1 ion-pair formation; and (iii), for concentrations above 0.11 mol $L^{-1}$ both considered complexation reactions i.e., 1:1 ion-pair formation and 2:1 H-bonding. The proposed model allowed thus to evaluate the relative importance of the phenomena occurring in the system in all the studied acid concentration range.

Keywords: organic acids, N,N-didodecylmethylamine (DDMA), apparent amine basicity, equilibrium modeling, infrared spectroscopy

## Nomenclature

| **Abbreviations** | **Meaning** | |
|---|---|---|
| 3-HP | 3-hydroxypropionic acid | |
| DDMA | N,N-didodecylmethylamine | |
| FT-IR | Fourier Transform Infrared spectroscopy | |
| MAE | Mean Absolute Error | |
| SE | Standard Error | |
| TOA | Trioctylamine | |
| **Symbol** | **Definition** | **Unit** |
| $[i]$ | $i$-species concentration in aqueous phase | mol $L^{-1}$ |
| $[\bar{\imath}]$ | $i$-species concentration in organic phase | mol $L^{-1}$ |
| Greek letters | | |
| $\beta$ | Apparent equilibrium constant | |
| $\delta$ | Bending vibrational mode | |
| $\varphi$ | Organic phase diluents to total volume ratio | - |
| $\nu$ | Stretching vibrational mode | |
| $K_a$ | 3-HP dissociation constant | mol $L^{-1}$ |
| $K_{11}$ | 1:1 ion pair complex formation constant | $L^2$ $mol^{-2}$ |
| $K_{21}$ | 2:1 complex formation constant | L $mol^{-1}$ |
| $K_{aq}$ | Side reaction constant | - |
| $K_m$ | Partition coefficient | - |
| $K_w$ | Water autoprotolysis constant | $L^2$ $mol^{-2}$ |
| $P_{o/w}$ | Octanol / water partition coefficient | - |
| $S$ | Sobol index | |
| $Y$ | Extraction yield | % |
| $Z$ | Loading ratio | mol $mol^{-1}$ |
| Subscripts/superscripts | | |
| $0$ | Initial concentration | |
| $aq$ | Relative to the aqueous phase | |
| $as$ | asymmetric stretch | |
| $eq$ | Total concentration at the equilibrium | |
| $exp$ | Experimental data | |
| $hn$ | Half-neutralization point | |
| $HPLC$ | Analytical concentration measured using High Performance Liquid Chromatography | |
| $org$ | Relative to the organic phase | |

| | |
|---|---|
| p | Number of acid molecules in the complex |
| $s$ | Symmetric stretch |
| $sim$ | Simulated data |
| $t$ | Total concentration |
| $T$ | Total Sobol indices |

## 1. Introduction

Due to growing concerns about climate change and the dependence on fossil resources [1], there is an increasing interest in the substitution of crude oil derivatives by bio-based products obtained from renewable feedstocks [2]. Historically, organic acids have been widely used in industry. The bioeconomy context has reinforced the interest in their production through biotechnological routes from renewable resources, for the development of bio-based materials [3]. Carboxylic acid biological production is inhibited by acid accumulation during the process, limiting both its productivity and titer. The inhibition can be alleviated by the implementation, among other techniques, of *In Situ* or In Stream Product Recovery (ISPR) processes. On the subject of extractive production of carboxylic acids, reactive liquid-liquid extraction has been extensively studied due to its high selectivity even at low acid titers, mild operation conditions, the possibility of continuous extractant regeneration and its low energy consumption [4,5].

Several extractants have been studied for the recovery of organic acids in literature. Kertes and King [6] classified the different extractants into (i) carbon-bonded oxygen-donor, (ii) phosphorous-bonded oxygen-donor and (iii) high molecular weight aliphatic amines. Among the diversity of extractants suitable for this application, tertiary aliphatic amines solubilized in organic solvents are the most common. Tertiary amines are highly hydrophobic molecules that interact with the acid present in aqueous phase through successive reversible complexation reactions at the liquid-liquid interface. The distribution ratios that can be achieved using tertiary amines are usually higher than those obtained with other extractants when the organic phase is properly formulated [7]. As amines show poor solvating properties, the formulation of organic phases generally includes an active diluent such as long-chain alcohols, capable of strongly solvating the acid-amine complexes through polar interactions (e.g. formation of H-bonds) [8].

3-hydroxypropionic acid (3-HP) emerged as one of the most promising chemical building blocks for the production of acrylic acid, biopolymers, and other chemicals with a wide range of applications in industry [9–11]. In this context, the interest in microbial production of 3-HP has increased in the last years [12,13]. 3-HP recovery

from microorganisms culture broths is still challenging because of the hydrophilic nature of this molecule ($\log P_{o/w} = -0.89$) and the low titers reached in the process($< 10\%$ w/w) due to low pH and acid inhibition [14]. This is why the implementation of reactive liquid-liquid extraction shows encouraging prospects.

The main drawback of reactive liquid-liquid extraction as ISPR technique remains the toxicity of the extraction phases in close contact with culture media. Recently, several studies have been published on the screening and formulation of organic phases accounting for the biocompatibility with some bacteria of the genus *Lactobacillus* [15,16]. In spite of the identification of more biocompatible organic phases, most experimental and equilibrium modeling studies so far focused on trioctylamine (TOA) or the commercially available Alamine 336 (a blend of $C_8$ and $C_{10}$ trialkylamines) in different mixtures of active and inert diluents, which are mostly deleterious for microorganisms.

The objective of this work is thus to propose an equilibrium model of the extraction of 3-hydroxypropionic acid using a new formulation of organic phase that has been identified from literature to be more biocompatible than other organic phases employed for 3-HP extraction [15,17]. Among promising biocompatible organic phases, we chose to focus on N,N-didodecylmethylamine (DDMA) diluted in a mixture of 1-dodecanol and dodecane as active and inactive diluent, respectively, according to the recent study of Sánchez-Castañeda et al. [15]. The authors found that DDMA showed better performances than TOA in terms of distribution coefficient as well as biocompatibility towards the natural 3-HP producer microorganism *Lactobacillus reuteri*. They attributed better extraction performances to the reduction of steric hindrance for reacting with acid molecules, while biocompatibility was linked to more hydrophobic nature of DDMA. The inclusion of long chain aliphatic alcohols as active diluents improved extraction performance. Nevertheless, depending on the chain length, primary alcohols could increase toxicity. As was the case for extractants, diluents' biocompatibility was found to be related to hydrophobicity, longer carbon chains being less toxic. The inclusion of alkanes as inert diluents was found to decrease extraction yield but was useful to further reduce toxicity, improving mass transfer. Thus, the authors concluded that the organic phase containing DDMA

diluted in 1-dodecanol and dodecane presented the best trade-off between extraction yield and biocompatibility.

In order to elucidate the underlying 3-HP extraction mechanisms, a set of extraction equilibrium experiments was performed at different initial acid concentrations. Fourier Transform Infrared spectroscopy (FT-IR) of loaded organic phases was employed as a means to understand the nature of acid-amine interactions. In order to validate and quantify the extraction mechanisms, a model built on the law of mass action, considering different acid-amine interactions was developed and its parameters were calibrated based on experimental data. The distribution of acid species in the organic phase was thus studied. A global sensitivity analysis of the model was ultimately performed through the estimation of main and total Sobol indices. The sensitivity analysis quantified the importance of each parameter in different acid concentration ranges and supported the discussion of the relative importance of the considered mechanisms.

## 2. Materials and Methods

### 2.1. Chemicals

3-Hydroxypropionic acid (CAS number 503-66-2) was purchased from TCI-Europe (Zwijndrecht, Belgium) as a 29.1% w/w solution in water. This solution was used to prepare all the solutions of the studied concentration range. N,N-didodecylmethylamine (DDMA, CAS number 2915-90-4, 98.1% purity) was purified as detailed in 2.2 and then diluted in 1-dodecanol (CAS number 112-53-8, 99% purity) and dodecane (CAS number 112-40-3, 99.5% purity), all three from TCI-Europe. Sulfuric acid (CAS number 7664-93-9, 95%) was purchased from Sigma-Aldrich (St. Louis, USA) and sodium hydroxide in aqueous solution (CAS number 1310-73-2, 35% w/w) from VWR Chemicals (Leuven, Belgium).

### 2.2. Amine purification

The commercial DDMA was purified by several steps of acid-base washing. Equal volumes of commercial amine and aqueous $H_2SO_4$ 0.1 mol $L^{-1}$ were vigorously mixed for 5 minutes and centrifuged during 1 h at 11 000 *g* and 25°C. The organic phase was then recovered and washed with equal volume of NaOH 0.3 mol $L^{-1}$ before being

centrifuged at 11 000 *g* for 20 minutes. These steps were done twice. The resulting organic phase was washed twice with Milli-Q ultrapure water and centrifuged for 1 h at 11 000 *g*. The purified DDMA was diluted to 20% v/v (0.45 mol $L^{-1}$) in 1-dodecanol (40% v/v) and dodecane (40% v/v) and used as organic extraction phase.

### 2.3. Extraction equilibrium experiments

Physical extraction experiments were performed by putting in contact 25 mL of aqueous phases containing 3-HP in concentrations ranging from 0.0056 to 0.28 mol $L^{-1}$ with equal volume of an organic phase consisting in 50% v/v 1-dodecanol and 50% v/v dodecane. The sample flask containing both phases was slightly mixed by gentle shaking for 5 minutes and then settled to reach the equilibrium for 72 h at 25°C. After equilibration, acid concentration in the aqueous phase was analyzed by HPLC and acid concentrations in organic phase were estimated through a mass balance. The partition coefficient was determined as the slope of the regression line of the graph of acid concentration in the organic phase versus acid concentration in the aqueous phase (Figure A1). Reactive extraction was evaluated by performing the same phase contacting protocol as for physical extraction. A volume of 2 mL of aqueous 3-HP phases solutions ranging from 0.0028 to 1 mol $L^{-1}$ was put in contact with equal volume of an organic phase containing 20% v/v purified DDMA, 40% v/v 1-dodecanol and 40% v/v dodecane. Under these mild contacting conditions, the formation of a stable emulsion difficult to separate was avoided. The time required to reach equilibrium inside the flask was determined through a preliminary experiment (not shown) and was found to be around 24 h. After reaching the equilibrium, the aqueous phase was analyzed by HPLC and its equilibrium pH was measured using a Mettler Toledo SevenCompact pH meter (Greisensee, Switzerland), equipped with a Mettler Toledo InLab Viscous Pro-ISM probe (Greisensee, Switzerland). The loaded extraction phase was recovered for FT-IR analysis. Each experiment was performed in triplicate and the reported concentrations and FT-IR spectra are averages. The extraction yield based on aqueous phase analysis was defined as Eq. (1):

$$Y_{exp} = \frac{[AH]_0^{HPLC} - [AH]_{eq}^{HPLC}}{[AH]_0^{HPLC}} \times 100\% \qquad (1)$$

### 2.4. Analytical methods

The concentration of 3-hydroxypropionic acid in aqueous phases was measured by High-Performance Liquid Chromatography (HPLC) using a Biorad Aminex HPX-87H column (CA, USA). The mobile phase used was 0.5 mmol $L^{-1}$ $H_2SO_4$ at a flowrate of 0.4 mL $min^{-1}$. The temperature was set at 65 °C. The samples were detected by a 210 nm UV detector.

### 2.5. FT-IR spectra acquisition

A drop (~20 µL) of the liquid sample to analyze was enclosed between two $CaF_2$ windows (ISP Optics, Riga, Latvia). IR spectra of the samples were recorded using a Nicolet Magna-IR 750 spectrometer (MA, USA) in the mid-IR region (wavenumbers between 800 and 4000 $cm^{-1}$) at ambient temperature. The resolution of the spectra was set to 2 $cm^{-1}$.

Gaussian peak deconvolution was performed using the *Multiple peak fit* tool in Origin 2021b software (OriginLab Corporation, MA, USA).

### 2.6. Amine basicity quantification

The amine basicity was estimated by determining the amine half-neutralization point as described by Canari and Eyal [18]. The cited method for determining the strength of highly hydrophobic amines was first introduced by Grinstead and Davis [19] as an analogy to acid-base equilibria in aqueous media. This method is based on the complete reaction of tertiary amines diluted in an organic phase after equilibration with aqueous hydrochloric acid, as expressed by Eq. (2).

$$\overline{R_3NH^+Cl^-} \overset{K_{a,B}}{\rightleftharpoons} \overline{R_3N} + H^+ + Cl^- \; ; \; K_{a,B} = \frac{[\overline{R_3N}][H^+][Cl^-]}{[\overline{R_3NH^+Cl^-}]} \qquad (2)$$

From Eq. (2) it is possible to define $\mathrm{p}K_{a,B}$ as Eq. (3):

$$\mathrm{p}K_{a,B} = -\log\left(\frac{[\overline{R_3N}]}{[\overline{R_3NH^+Cl^-}]}\right) + \mathrm{pH} - \log([Cl^-]) \qquad (3)$$

The half-neutralization point corresponds to the point where half of the amine in the organic phase is neutralized by hydrochloric acid. Hence, at the half-neutralization point $[\overline{R_3N}]_{hn} = \left[\overline{R_3NH^+Cl^-}\right]_{hn}$, and $\mathrm{p}K_{a,B}$ is given by Eq. (4):

$$\mathrm{p}K_{a,B} = \mathrm{pH_{hn}} - \log([Cl^-]) \qquad (4)$$

Aiming to measure the pH at the half-neutralization point, a volume of 1 mL of organic phase was put in contact with HCl 1 mol $L^{-1}$ in an acid/amine molar ratio of 1:1. After 72 h of contact, NaOH 0.5 mol $L^{-1}$ was added to the aqueous phase in an acid/base ratio of 2:1. The resulting pH of the aqueous phase recovered corresponds to $\mathrm{pH}_{hn}$.

## 3. Theory

At the standard state (pure liquid at 25 °C), reactive liquid-liquid extraction of 3-HP using DDMA involves several physicochemical phenomena, namely physical partitioning, self-ionization of water, acid dissociation, reactive extraction by tertiary amine, electroneutrality and organic impurities impact. All these phenomena are considered below for modeling purposes.

### 3.1. Physical partitioning

When aqueous 3-HP phases are in contact with an organic phase containing an extractant, almost all the acid transferred to the organic phase is extracted as acid-extractant complexes (reactive extraction). Nevertheless, a small part of the acid is present in the organic phase as a result of physical partitioning with the organic phase diluents, leading to the definition of the partition coefficient $K_m$ introduced in Eq. (5).

$$AH \overset{K_m}{\rightleftharpoons} \overline{AH}\,;\; K_m = \frac{[\overline{AH}]}{\varphi[AH]} \qquad (5)$$

where $[\overline{AH}]$ represents the concentration of total free acid in the organic phase, which is extracted by neat diluents, and $[AH]$ the total acid concentration in aqueous

phase. As the organic phase's total volume contains also the extractant, it is necessary to take into account the diluent's fraction $\varphi$ expressed in Eq. (6).

$$\varphi = \frac{V_{diluents}}{V_{org\ phase}} \qquad (6)$$

### 3.2. Self-ionization of water

The equilibrium between hydronium and hydroxide ions in solution is determined by the auto-ionization constant of water. This equilibrium is presented in Eq. (7):

$$H_2O \overset{K_w}{\rightleftharpoons} OH^- + H^+ ;\ K_w = [OH^-][H^+] \qquad (7)$$

### 3.3. Acid dissociation

For a weak acid in an aqueous medium, the distribution of the undissociated and dissociated species is given by its dissociation constant $K_a$, presented in Eq. (8):

$$AH \overset{K_a}{\rightleftharpoons} A^- + H^+ ;\ K_a = \frac{[A^-][H^+]}{[AH]} \qquad (8)$$

Based on the hydronium ion concentration (Eqs. (7-8)), pH in aqueous phases is defined as:

$$\mathrm{pH} = -\log[H^+] \qquad (9)$$

### 3.4. Complexation reactions by a tertiary amine

Reactive extraction of 3-HP is achieved through a set of reversible complexation reactions taking place between the acid in the aqueous phase and the tertiary amine in the organic phase. As reported by different authors ([20,21]), when the amine basicity is high enough to bind a proton, the formed cation interacts with the dissociated acid in aqueous phase to form a complex with 1:1 stoichiometry soluble in the organic phase. This mechanism is known as ion pair formation. The global reaction mechanism is presented in Eq. (10):

$$A^- + H^+ + \overline{R_3N} \overset{K_{11}}{\rightleftharpoons} \overline{CPX_{11}} ;\ K_{11} = \frac{\left[\overline{CPX_{11}}\right]}{[A^-][H^+]\left[\overline{R_3N}\right]} \qquad (10)$$

For simplification purposes, $R_3$ represents three generic alkyl groups, possibly different from each other. In the case of DDMA, $R_3 = R_2R'$, where $R$ represents a dodecyl group and $R'$ represents a methyl group.

At high initial acid concentrations, an undissociated acid molecule can interact with the 1:1 complex by hydrogen bonding thus forming a 2:1 complex.

$$AH + \overline{CPX_{11}} \overset{K_{21}}{\rightleftharpoons} \overline{CPX_{21}};\ K_{21} = \frac{[\overline{CPX_{21}}]}{[\overline{CPX_{11}}][AH]} \qquad (11)$$

In the same manner as 2:1 complex formation, higher stoichiometry complexes could be formed through successive aggregation of acid molecules. This phenomenon depends on the acid nature, the extractant and the interaction between both of them. Considering that 1:1 complex is formed by ion-pairing, the global reaction of higher stoichiometry complexes can be described as Eq. (12):

$$A^- + H^+ + (p-1)\,AH + \overline{R_3N} \overset{\beta_{p1}}{\rightleftharpoons} \overline{CPX_{p1}};\ \beta_{p1} = \frac{[\overline{CPX_{p1}}]}{[\overline{R_3N}][A^-][H^+][AH]^{(p-1)}} \qquad (12)$$

where $\beta_{p1} = \prod_{n=1}^{p} K_{n1}$

Complexes containing more than one amine molecule can also be formed in some cases but are not considered in this work as this mechanism is likely to occur only for secondary amines [21].

The global extraction yield presented in Eq. (13) is defined as the ratio of all acid species in the organic phase and the initial acid concentration in the aqueous phase.

$$Y = \frac{[\overline{AH}] + \sum_{n=1}^{p} n\,[\overline{CPX_{n1}}]}{[AH]_0} \frac{V_{org}}{V_{aq}} \times 100\% \qquad (13)$$

### 3.5. Mass balances

The mass balances of the acid and the tertiary amine are given by Eqs (14) and (15)

$$[AH]_0 = [AH] + [A^-] + \frac{V_{org}}{V_{aq}}\left([\overline{AH}] + \sum_{n=1}^{p} n\,[\overline{CPX_{n1}}]\right) \quad (14)$$

$$[\overline{R_3N}]_0 = [\overline{R_3N}] + \sum_{n=1}^{p} [\overline{CPX_{n1}}] \quad (15)$$

### 3.6. Amine loading ratio

The reactive extraction of the acid by a tertiary amine can be characterized using the loading ratio $Z$. The loading ratio of the extractant is defined as the ratio between the total concentration of acid in the organic phase (extracted by the amine) and the initial concentration of amine in the organic phase. The loading ratio is a function of the strength of the acid-amine interaction, the stoichiometry of the overall equilibrium reactions and the initial acid and extractant concentrations [22].

The general expression of the loading ratio is given by Eq. (16):

$$Z = \frac{\sum_{n=1}^{p} n\,[\overline{CPX_{n1}}]}{[\overline{R_3N}]_0} \quad (16)$$

When $p = 1$, i.e., ion-pair 1:1 complex formation, $Z$ is defined as Eq. (17):

$$Z = \frac{[\overline{CPX_{11}}]}{[\overline{R_3N}]_0} \quad (17)$$

Combining Eq. (10), (15) and (17):

$$\frac{Z}{1-Z} = K_{11}[A^-][H^+] \quad (18)$$

If reactive extraction follows ion-pair 1:1 complex formation, the plot of $Z/(1-Z)$ versus $[A^-][H^+]$ yields a straight line with slope equal to $\mathrm{K}_{11}$.

For the general case of the formation of higher stoichiometry complexes, if $\left[\overline{CPX_{p1}}\right] \gg \left[\overline{CPX_{i1}}\right]; i \neq p$, $Z$ can be simplified as given in Eq. (19):

$$Z \cong \frac{p\left[\overline{CPX_{p1}}\right]}{\left[\overline{R_3N}\right]_0} \qquad (19)$$

Combining Eq. (12), (15) and (19):

$$\beta_{p1}[A^-][H^+][AH]^{(p-1)} \cong \frac{Z}{p-Z} \qquad (20)$$

Consequently, the plot of $Z/(p-Z)$ versus $[A^-][H^+][AH]^{(p-1)}$ is a straight line with slope $\beta_{p1} = \prod_{n=1}^{p} K_{n1}$, if the main assumption of predominance of $\left[\overline{CPX_{p1}}\right]$ is valid.

### 3.7. Electroneutrality principle

Considering that there is no net charge in the aqueous phase, the sum of the concentration of positively charged species is equal to the sum of the concentrations of negatively charged species:

$$[A^-] + [OH^-] = [H^+] \qquad (21)$$

## 4. Modeling Reactive Liquid-Liquid Extraction

### 4.1. Organic impurities impact

As a result of their synthesis process (alkylation of primary amines), commercial tertiary amines contain unreacted primary and secondary amines [23]. These lower amines, considered as impurities, are more soluble in water than tertiary amines and have an effect on the pH and the extraction yield. In order to model the effect of organic impurities on the extraction, a neutralization reaction was considered to occur between a pseudo-species $\overline{RNH_2}$, representing organic impurities (primary amines), and the undissociated acid. Impurities involved in the considered side reaction are solubilized into the aqueous phase. Eq (22) presents the side reaction:

$$\overline{RNH_2} + AH \overset{K_{aq}}{\rightleftharpoons} RNH_3^+ + A^-\ ;\ K_{aq} = \frac{[RNH_3^+][A^-]}{\left[\overline{RNH_2}\right][AH]} \qquad (22)$$

The mass balance for impurities can be defined as Eq. (23):

$$\left[\overline{RNH_2}\right]_0 = \left[\overline{RNH_2}\right] + \frac{V_{aq}}{V_{org}}[RNH_3^+] \qquad (23)$$

Given that a new positively charged species is introduced in the aqueous phase, the electroneutrality principle is modified as stated in Eq. (24):

$$[A^-] + [OH^-] = [H^+] + [RNH_3^+] \qquad (24)$$

### 4.2. Numerical solution of the mathematical models

Three different models of increasing complexity were compared in this study: firstly, a model considering 1:1 complex formation and neglecting the presence of impurities, secondly, the formation of a 2:1 complex was added to the first model, and finally, a model including 1:1 and 2:1 complexes and the side reaction. Table 1. presents the model equations, their parameters and their calibration datasets.

**Table 1.** Definition of the three considered models.

| | Model | Equations | Parameters | Calibration datasets |
|---|---|---|---|---|
| 1 | 1:1 stoichiometry model ($p$ =1) without impurities | (5), (7)-(8), (10), (14)-(15), (21) | $K_{11}$ | Extraction yield |
| 2 | 1:1 stoichiometry model ($p$ =1) + 2:1 stoichiometry model ($p = 2$) without impurities | (5), (7)-(8), (10)-(11), (14)-(15), (21) | $K_{11}, K_{21}$ | Extraction yield |
| 3 | 1:1 stoichiometry model ($p$ =1) + 2:1 stoichiometry model ($p = 2$) including impurities | (5), (7)-(8), (10)-(11), (14)-(15), (22)-(24) | $K_{11}, K_{21}, K_{aq}$ and $[\overline{RH_2N}]_0$ | Extraction yield Equilibrium pH |

The parameters of models 1 and 2 were calibrated using the extraction yield measured in the experimental section, by minimizing the difference between measured and calculated values in the least-squares sense. For model 3, measured equilibrium pH was also included as a calibration data set because one of the main

consequences of the side reaction was pH increase, compared to the theoretical values without impurities. The values of the two experimental datasets were divided by their respective ranges of variation in order to obtain values of similar order of magnitude suitable for simultaneous use in parameter calibration. Given that the correlation between $K_{aq}$ and $[\overline{RH_2N}]_0$ was greater than 98%, it was not possible to estimate the two parameters simultaneously. For this reason, an external loop was implemented to make $[\overline{RH_2N}]_0$ vary between 0.5 and 5 mmol $L^{-1}$. For each fixed $[\overline{RH_2N}]_0$, parameters $K_{11}$, $K_{12}$ and $K_{aq}$ were determined. The combination of parameters giving the best fit was selected among the solutions significantly different from zero (i.e. zero was not included in the 95% confidence interval of either parameter).

The goodness of fit of the proposed models has been evaluated using the mean absolute error (MAE), defined as Eq. (25)

$$MAE = \frac{1}{N}\sum_{k=1}^{N}\left|y_{exp} - y_{sim}\right| \qquad (25)$$

where $N$ is the number of experimental points, $y_{exp}$ are the observed values and $y_{sim}$ the predicted values.

MATLAB R2020b (The MathWorks Inc., Natick, MA), equipped with Statistics and Optimization toolboxes was used for numerical calculations. For each model, the systems of nonlinear equations listed in Table 1 were solved with the 'trust region' algorithm implemented in the *fsolve* function. The *nlinfit* function implementing the Levenberg-Marquardt algorithm was used to solve the nonlinear least-squares problem for parameter estimation. The values of the fixed parameters for calculations are listed in Table 2.

**Table 2.** Fixed parameters for calculations

| Parameter | Value | Unit | Present in Eq. |
|---|---|---|---|
| $\varphi$ | $0.8$ | - | (5)-(6), (13)-(14) |
| $K_a = 10^{-pK_a\star}$ | $3.09 \times 10^{-5}$ | $\mathrm{mol\ L^{-1}}$ | (8) |
| $K_w$ | $10^{-14}$ | $\mathrm{L^2\ mol^{-2}}$ | (7) |
| $K_m$** | $0.004$ | - | (5) |

| | | | |
|---|---|---|---|
| $[\overline{R_3N}]_0$ | 0.45 | mol $L^{-1}$ | (15)-(17), (19) |
| $V_{aq}$ | $2 \times 10^{-3}$ | L | (14), (23) |
| $V_{org}$ | $2 \times 10^{-3}$ | L | (14), (23) |

* Taken from [24]

** Described in sec. 2.3 (Figure A1 in appendices).

### 4.3. Sensitivity analysis

Global Sensitivity Analysis was performed through the estimation of Sobol indices as described by Jansen [25] and Saltelli et al. [25]. For each initial acid concentration, the model was solved $N = 5 \times 10^4$ times with random parameter sets drawn from a normal distribution with standard deviation equal to 10 % of the mean estimated value of each parameter. Confidence intervals for Sobol indices were estimated using the bootstrap method.

## 5. Results and discussion

### 5.1. Experimental results: extraction yield and equilibrium pH

Table 3 and Figure 1 present the experimental yield, the observed equilibrium pH and loading ratios obtained from the equilibrium experiments described in section 2.3.

**Table 3.** Experimental equilibrium results

| Initial acid concentration (mol $L^{-1}$) | Extraction yield (%) | Equilibrium pH (-) | Loading ratio (mol $mol^{-1}$) |
|---|---|---|---|
| 0.0028 | 20.50 | 4.99 | 0.003 |
| 0.0054 | 37.23 | 4.36 | 0.008 |
| 0.0082 | 44.41 | 3.89 | 0.012 |
| 0.011 | 44.90 | 3.71 | 0.015 |
| 0.022 | 47.15 | 3.52 | 0.027 |
| 0.054 | 47.71 | 3.36 | 0.062 |
| 0.082 | 48.14 | 3.24 | 0.092 |
| 0.11 | 53.62 | 3.09 | 0.138 |
| 0.22 | 54.75 | 2.91 | 0.278 |
| 0.34 | 57.63 | 2.88 | 0.437 |

| | | | |
|---|---|---|---|
| 0.45 | 55.83 | 2.79 | 0.561 |
| 0.57 | 52.78 | 2.72 | 0.670 |
| 0.65 | 50.75 | 2.61 | 0.739 |
| 0.77 | 50.68 | 2.63 | 0.868 |
| 0.85 | 43.90 | 2.51 | 0.830 |
| 1.0 | 42.38 | 2.48 | 0.929 |

The extraction yield measured experimentally varied between 40% to 60% in all the studied concentration range except for concentrations lower than 0.008 mol $L^{-1}$, for which the observed yield is lower. This behavior has already been observed by some authors [27,28] and is generally related to the presence of impurities originated in commercial tertiary amines synthesis process. Impurities consist mainly in traces of primary amines as mentioned previously. Primary amines are less hydrophobic than tertiary amines (e.g. $\mathrm{Log}\, P_{o/w} = 3.06$ for octylamine and $\mathrm{Log}\, P_{o/w} = 10.94$ for TOA) and have a negative impact on the extraction performance by reacting with the acid in the aqueous phase. The availability of acid molecules to reactive extraction into the organic phase is thus decreased and its effect is especially noticeable at acid concentrations low enough to be comparable to the concentration of primary amines in the organic phase.

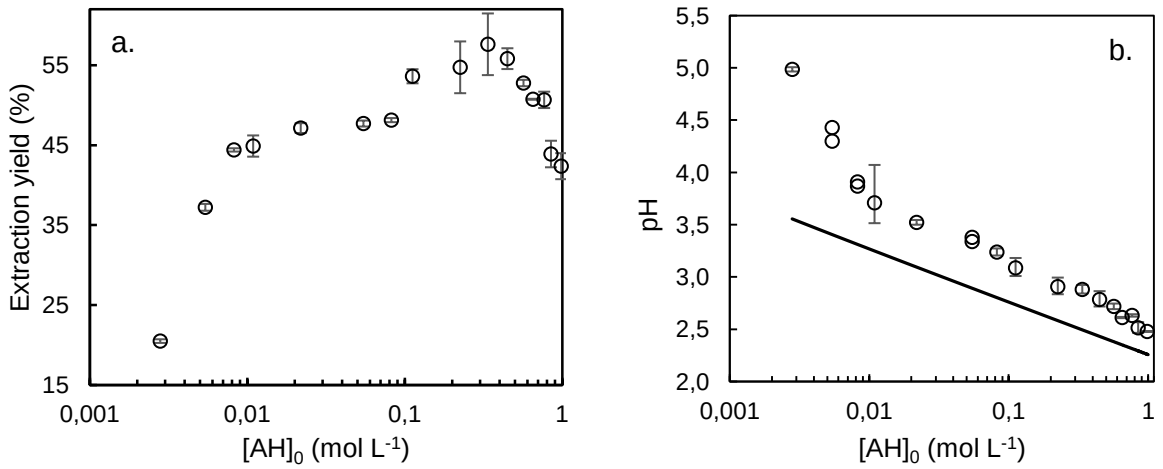


**Figure 1.** Experimental results as a function of initial 3-HP concentration a. Extraction yield, b. Equilibrium pH: experimental (symbols), theoretical (solid line). Error bars represent standard deviation

This problem was illustrated by Kaur and Elst [27] by studying the reactive extraction of itaconic acid with several amines in many diluents. They reported that the most

effective extractants were the most hydrophobic ones. Inversely, the less hydrophobic extractants showed poor extraction yields. As an example of this, those authors found that the distribution ratio obtained using TOA in 1-decanol was almost 8 times higher than that using octylamine in the same diluent. These results were attributed to the partial solubility of primary amines in the aqueous phase that decreased their availability for acid extraction into the organic phase. Chemarin et al. [28] obtained similar results for 3-HP extraction using TOA diluted in 1-decanol. They found that in presence of octylamine in the organic phase at concentrations near 2 mmol $L^{-1}$, the extraction yield of 3-HP decreased from 70% to 10% for initial acid concentrations lower than 0.1 mol $L^{-1}$. They proposed the acid-base purification protocol presented in 2.2 and obtained a purified TOA containing less than 0.06 mmol $L^{-1}$ octylamine. The organic phase prepared using purified TOA showed no decrease in extraction yield at lower acid concentrations. In the present study, although DDMA was purified using the same protocol, the decrease in the extraction yield was still observed at lower acid concentrations, suggesting that DDMA purification was not optimal. Therefore, further studies need to be conducted to precisely quantify the impurities in commercial DDMA aiming to design a more adapted purification protocol.

The transfer of amine impurities to the aqueous phase also had an effect on the equilibrium pH [29]. It can be observed that experimental pH measured at equilibrium is indeed systematically higher than the theoretical pH estimated considering the 3-HP concentration at equilibrium measured by HPLC (Figure 1b). The discrepancy is especially high for acid concentrations below 0.008 mol $L^{-1}$.

In the range 0.08 mol $L^{-1}$ – 0.11 mol $L^{-1}$ the extraction yield seemed to reach a plateau and increased again for $[AH]_0 > 0.11$ mol $L^{-1}$ with a maximum reached at 0.45 mol $L^{-1}$ (Figure 1a). This behavior could indicate that the reactive extraction in all the studied range is the combination of different acid-amine interactions. When initial acid concentrations are high enough ($Z > 0.5$), which corresponds to $[AH]_0$ higher or equal to 0.45 mol $L^{-1}$ (Table 3), it is considered that more than one acid molecule is complexed by the amine [30].

### 5.2. Nature of 3-HP-DDMA complex: an FT-IR spectroscopy study

In order to gain insights into the interactions between 3-HP molecules and amine in the organic phase, several IR spectra were recorded. This section presents the analysis of the FT-IR spectra of loaded extraction phases and results are further used to support the mechanistic model of reactive liquid-liquid extraction of 3-HP using DDMA in 1-dodecanol/dodecane. FT-IR spectra of different compounds used in this study are presented in the appendices section.

#### 5.2.1. Organic acids characteristic IR bands

The spectral analysis of samples containing organic acids is particularly interesting in the region 1100 – 1800 $cm^{-1}$ in which several carbonyl/carboxyl characteristic bands of organic acids appear. As an example, Figure 2 presents FT-IR spectra of commercial 3-HP aqueous acid and the same product neutralized with NaOH. pH of the commercial 3-HP solution (3.2 mol $L^{-1}$) is about 2.0, consequently more than 99% of the acid is in its undissociated form (estimated using Equation (8)). This product showed a strong absorption peak at about 1720 $cm^{-1}$. The region comprising 1700 – 1780 $cm^{-1}$ corresponds to carbonyl stretch ($\nu(C=O)$) in a carboxyl functional group and has been extensively linked to the presence of undissociated forms of organic acids [31]. When this region is present at lower wavenumbers (1700 – 1720 $cm^{-1}$), carbonyl groups are considered to be involved in hydrogen bonds. In certain cases, they are associated to acid molecules forming cyclic dimers although cyclization has not been yet proved by means of FT-IR data [32].

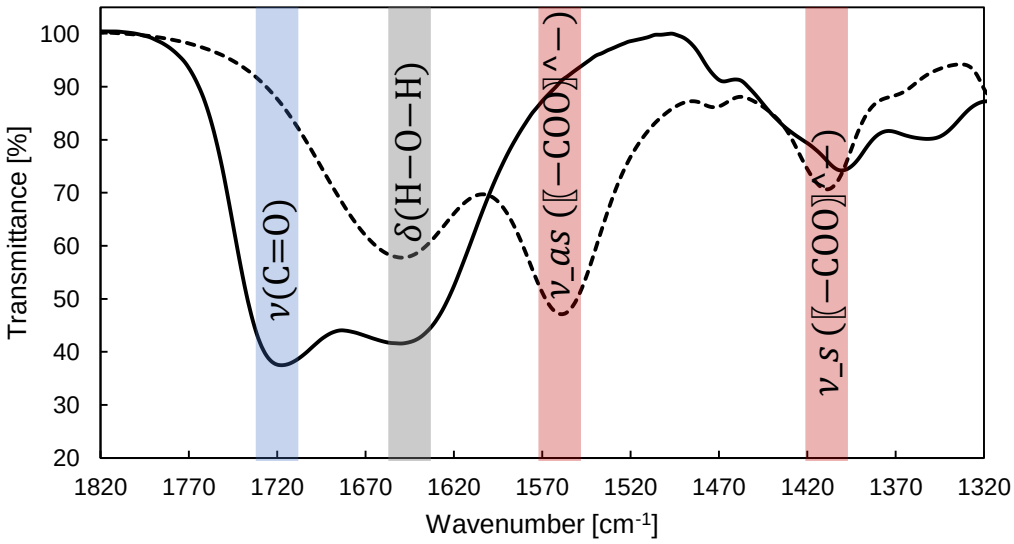


**Figure 2.** FT-IR spectra of 3-HP in solution (3.2 mol $L^{-1}$)
Commercial product (solid line), Commercial product neutralized with NaOH (dashed line)

Regarding neutralized 3-HP (pH = 7, more than 99% dissociated), spectra lack a peak in the 1700 – 1720 $cm^{-1}$ region. Instead, a peak in the region 1550 – 1620 $cm^{-1}$ appeared. In this case, the peak at about 1565 $cm^{-1}$ is assigned to the asymmetric stretch of the carboxylate group ($\nu_{as}(\mathrm{COO^-})$) and hence attributed to the presence of dissociated acid molecules [31]. A common peak between the two solutions could be found at about 1650 $cm^{-1}$ and is related to the bending of water molecules in the sample ($\delta(\mathrm{H-O-H})$).

### 5.2.2. Loaded organic phases

In the light of the previously described absorption bands, a similar analysis was done for the loaded extraction phases aiming to elucidate the nature of the acid-amine interaction. FT-IR spectra of some loaded organic phases are presented in Figure 3. As it can be observed, all the spectra of loaded extraction phases present a peak at 1571 $cm^{-1}$. This indicates the presence of the acid in its dissociated form and thus that the acid forms an ion-pair with the amine in the organic phase. This mechanism has been reported to be mostly dependent on the basicity (strength) of the extractant in the diluents, the dissociation constant of the acid and its hydrophobicity (for 3-HP, $\mathrm{p}K_a = 4.51$, $\log P_{o/w} = -0.89$) [33].

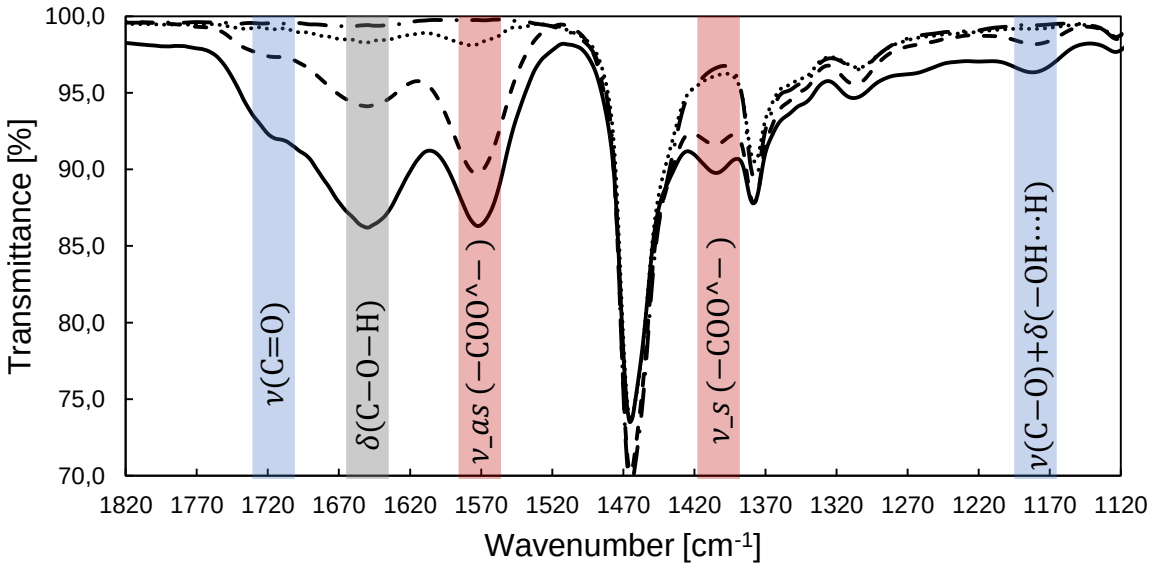


**Figure 3**. FT-IR spectra of organic extraction phases after prior equilibration with aqueous 3-HP solutions at different initial concentrations. $[AH]_0$: 0.01 mol $L^{-1}$ (dashdotted line), 0.11 mol $L^{-1}$ (dotted line), 0.55 mol $L^{-1}$ (dashed line), 1 mol $L^{-1}$ (solid line)

Due to the difficulty of estimating acid-base properties of water-insoluble tertiary amines diluted in organic phases, it is convenient to define an apparent basicity with respect to the equilibrium with protons in the aqueous phase. The apparent basicity of a given amine in given diluents depends on amine properties (substituents, steric hindrance), diluents' properties (polarity, proton donor or acceptor) and the extracted acid [18]. Canari and Eyal [34] proposed an equilibrium constant $\mathrm{p}K_{a,B}$ of the reaction of the tertiary amine with HCl (section 2.6). Those authors stated that for amines with higher or similar basicity than the conjugated base of the acid to extract ($\mathrm{p}K_{a,B} \geq \mathrm{p}K_a$), ion-pairing is the predominant extraction mechanism.

The value of $\mathrm{p}K_{a,B}$ measured for the organic phase used in this study was found to be equal to $6.42 \pm 0.08$. According to these results, DDMA (20% v/v) in 1-dodecanol (40% v/v) and dodecane (40% v/v) is a stronger base than the conjugate base of 3-HP in the aqueous phase. The amine is strong enough to bind a proton and the dissociated acid form is therefore extracted in order to keep electroneutrality in the organic phase. The presence of a polar diluent, especially a protic solvent such as 1-dodecanol, plays an essential role in this mechanism by facilitating the solvation of ion-pairs in the organic phase by polar interactions [33].

Recently, Chemarin et al [35] proposed this mechanism for 3-HP extraction based on FT-IR data obtained using TOA in 1-decanol. Ion-pair formation has been widely studied for several organic acids using different tertiary amines [36–38].

For initial acid concentrations higher than 0.11 mol $L^{-1}$, spectra of loaded organic phases show a shoulder at about 1716 $cm^{-1}$. The apparition of this peak indicates the presence of the undissociated acid form in the organic phase, more particularly, carboxyl groups participating in H-bonds. Different explanations of this phenomenon can be formulated: (i) the presence of free acid extracted by physical partitioning, (ii) the existence of a tautomeric equilibrium between the ionic complex and a hydrogen-bonded form of this complex, and (iii) the formation of high stoichiometry complexes.

Concerning hypothesis (i), the presence of free acid molecules in the organic phase can be neglected due to the low partition coefficient of 3-HP in the organic phase diluents ($K_m = 0.004$). In the studied concentration range (0.0028 – 1 mol $L^{-1}$), the acid extracted by physical partitioning is so low that it is undetectable by FT-IR.

Regarding hypothesis (ii), the existence of an equilibrium between a complex formed by proton transfer and a molecular complex formed by hydrogen-bonding (see Figure 4) have been reported to happen in several acid-amine couples in different organic phases [21,39,40]. Gusakova et al. [41] recorded spectra from an equimolar mixture of isobutyric acid and triethylamine diluted in $C_2Cl_4$. They observed a decrease of the $\nu(\mathrm{C=O})$ band and an increase of $\nu_{as}(-\mathrm{COO^-})$ proportional to the addition of methanol (a polar and protic solvent). Hence, they concluded that tautomeric equilibrium is highly dependent on the diluents, and it is mostly shifted to the ion-pair form in presence of a polar solvent. These observations were also validated by the same authors using isobutyric acid in dimethyl sulfoxide and acetonitrile, both polar solvents. In this study, the presence of 1-dodecanol as a polar and protic diluent (40% v/v) would shift the equilibrium showed in Figure 4 to the ion-pair form of the complex.

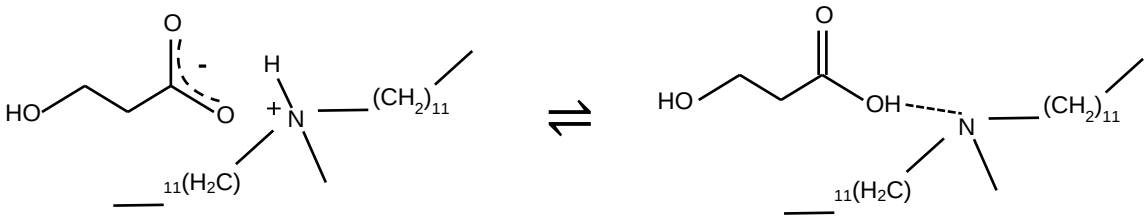


**Figure 4.** Tautomeric equilibrium of ionic and molecular 1:1 acid-amine complexes.

As discussed previously, hypothesis (i) and (ii) are unlikely to occur, consequently, the apparition of the shoulder at ~1716 cm$^{-1}$ can be attributed to hypothesis (iii), i.e., to the aggregation of undissociated acid molecules to the ion-pair complex through hydrogen bonding [42]. This seems to be in agreement with another phenomenon observed in spectra of loaded organic phases (Figure 3) for $[AH]_0 > 0.11$ mol L$^{-1}$: the apparition of a $C-O$ bond stretch band ($\nu(C-O)$) coupled with the scissoring of a hydrogen-bonded hydroxyl group ($\delta(-OH\cdots O)$) at 1189 cm$^{-1}$ [43]. The ratio between the surface of the $\nu(C=O)$ band at 1716 cm$^{-1}$ and $\nu(-COO^-)$ that at 1570 cm$^{-1}$ decreases while increasing initial concentration of 3-HP. For this reason, the formation of high stoichiometry complexes is considered to gain importance with respect to 1:1 ion-pair formation at higher acid concentrations. The structure of the different acid-amine complexes considered is presented in Figure 5.

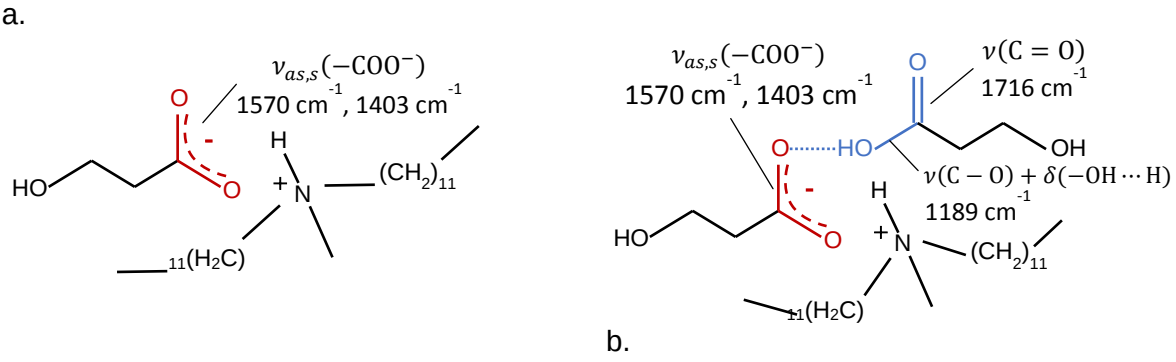


**Figure 5.** Proposed structures for acid-amine complexes and their characteristic IR bands
a.1:1 complex, b. 2:1 complex

### 5.2.3. Water co-extraction

All the loaded organic phases showed the characteristic peak of bending of water molecules at 1650 $cm^{-1}$. Tamada and King [44] observed water co-extraction in a set of reactive extraction experiments of several mono and dicarboxylic acids using Alamine 336 in different active diluents. They reported that this phenomenon was highly dependent on the solubility of free water molecules in active diluents. They also observed that monocarboxylic acids such as lactic and acetic acid carried less water than dicarboxylic acids, inferring that water molecules were tightly bound to the carboxylate part of organic acids. In this work, when the organic phase was priorly equilibrated with pure water, the observed water band is negligible (Figure 6) and it increases while increasing the initial acid concentration. Therefore, the presence of the water band in loaded organic phases is due to the co-extraction of water molecules bound to acid-amine complexes.

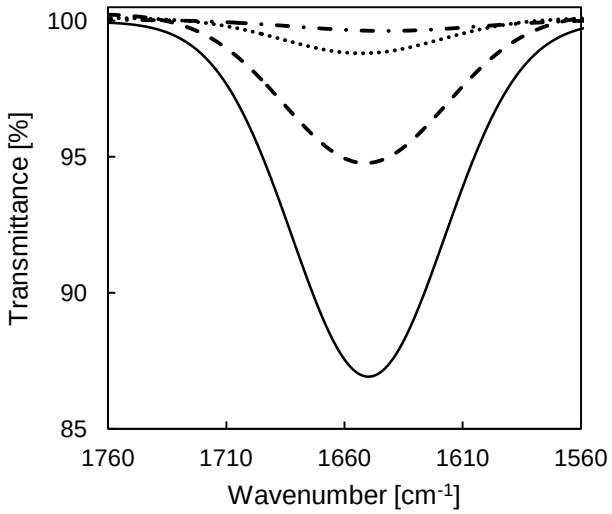


**Figure 6.** Deconvoluted water bands in loaded organic phases
Pure water (dashdotted line), organic phases after being equilibrated with 3-HP solutions:
0.11 mol $L^{-1}$ (dotted line), 0.55 mol $L^{-1}$ (dashed line), 1 mol $L^{-1}$ (solid line)

In Figure 6, a deconvolution of the peaks showed in Figure 3 was done for the sake of better data visualization than in the case of the overlapping peaks.

### 5.3. Modeling results

Figure 7 shows the predicted extraction yield and equilibrium pH for the three models,
calibrated based on experimental data. Table 4 presents the estimated parameters of each model. It appears that model 1 predicts a slight increase of the extraction yield while increasing initial acid concentrations until 0.02 mol $L^{-1}$. For higher concentrations, amine becomes the limiting reactant, and consequently, a strong decline is observed. Recall that Model 1 includes only the 1:1 acid-amine complex formation, and accordingly is unable to predict the behavior observed for acid concentrations exceeding 0.1 mol $L^{-1}$ (increase in yield) and below 0.08 mol $L^{-1}$ (strong yield decrease and high equilibrium pH). Model 1 shows thus poor accuracy for predictions of both extraction yield and equilibrium pH. In average, the absolute difference between predicted values and observed values is 0.11 in the case of the yield ($MAE_{yield} = 11\%$) and 0.34 pH units for equilibrium pH ($MAE_{pH} = 0.34$). Model 2 additionally includes the 2:1 acid-amine complex and captures the general trend of the extraction yield increase in the 0.08 – 0.3 mol $L^{-1}$ range and the subsequent decline from 0.3 mol $L^{-1}$. Nevertheless, model 2 is unable to describe the behavior of the extraction yield and equilibrium pH towards lower concentrations. The inclusion of the 2:1 complex formation improved the accuracy on the estimation of the extraction yield ($MAE_{yield} = 4.5\%$) but no significant improvement was observed in the prediction of the pH ($MAE_{pH} = 0.33$). Model 3 includes the side reaction with water soluble amines and captures correctly all the observed variations of the extraction yield and equilibrium pH in all the studied concentration range. This model was more accurate in the prediction of both the extraction yield ($MAE_{yield} = 2.5\%$) and the equilibrium pH ($MAE_{pH} = 0.15$). This model overestimates pH for initial acid concentrations between 0.008 and 0.02 mol L-1. As pointed out by sensitivity analysis (section 5.4), pH estimations are highly related to the considered parasite reaction. The parasite reaction presented in this work is a simplification of a series of acid-base reactions that could occur between acid molecules and different primary amines transferred from the organic phase to the aqueous phase. Even if the inclusion of the parasite reaction improved pH prediction, real phenomena are expected to be more complex than those considered in the model and cause a deviation from a behavior predicted using a single global pseudo-species.

Despite this simplification, model 3 accounted for the observed phenomena with satisfactory accuracy, in agreement with the extraction mechanism proposed in 5.2.2.

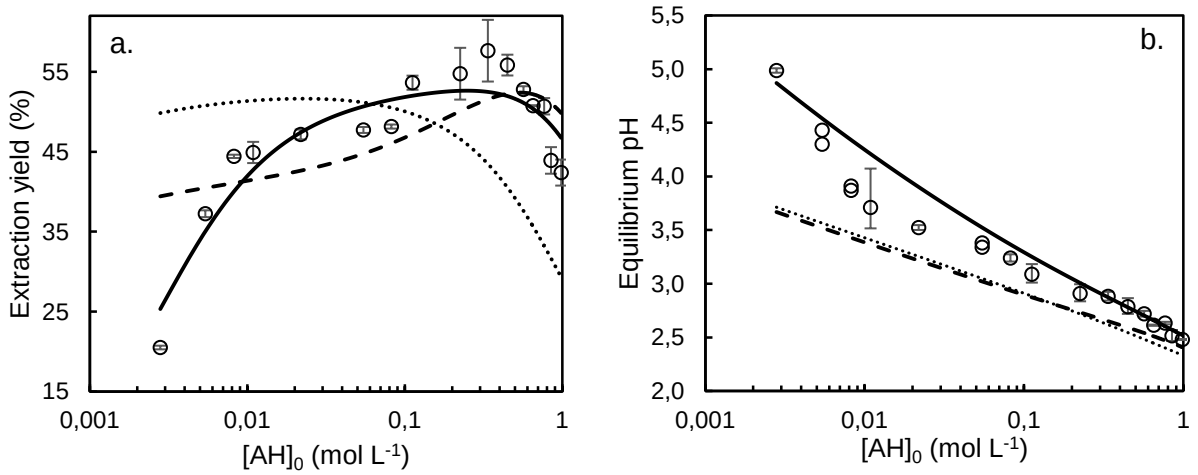


**Figure 7.** a. Extraction yield and b. equilibrium pH as a function of initial 3-HP concentration.
Experimental data (symbols), model 1 (dotted line), model 2 (dashed line), model 3 (solid line).
Error bars represent standard deviation

Model 3 complexation constants $K_{11}$ and $K_{21}$ were estimated with a reasonable uncertainty (less than 10 %). The uncertainty on the reaction constant estimation $K_{aq}$ is however higher because it represents the relatively minor side reaction of the acid with the global pseudo-species $\overline{RNH_2}$.

**Table 4.** Estimated parameters for the three proposed models

| Model | Parameters | Estimated value | Coefficient* of variation, CV (%) | Model accuracy | |
|---|---|---|---|---|---|
| | | | | $MAE_{yield}$ | $MAE_{pH}$ |
| 1 | $K_{11}$ ($L^2$ $mol^{-2}$) | $8.36 \times 10^4$ | 4.2% | 11% | 0.34 |
| 2 | $K_{11}$ ($L^2$ $mol^{-2}$) | $5.34 \times 10^4$ | 5.8% | 4.5% | 0.33 |
| | $K_{21}$ (L $mol^{-1}$) | 3.28 | 14.4% | | |
| 3** | $K_{11}$ ($L^2$ $mol^{-2}$) | $8.06 \times 10^4$ | 3.2% | 2.5% | 0.15 |
| | $K_{21}$ (L $mol^{-1}$) | 1.62 | 8.7% | | |
| | $K_{aq}$ (-) | 3.98 | 23.9% | | |

* $\mathrm{CV} = \frac{\text{Standard error of the estimation}}{\text{estimated value}} \times 100\%$

** for $[\overline{RH_2N}]_0 = 2 \times 10^{-3}$ mol $L^{-1}$

Impurities showed a clear effect on the extraction yield at very low acid concentrations ($[AH]_0 < 0.02$ mol $L^{-1}$) and a minor effect in the rest of the range. The inclusion of the side reaction significantly improved the prediction of the drop of the extraction yield and the gap between the predicted pH and the experimental pH at $[AH]_0 < 0.02$ mol $L^{-1}$.

The plot of the loading ratio as a function of the undissociated acid concentration in the aqueous phase at the equilibrium is shown in Figure 8. This curve is known as the loading curve. Experimental loading curves are generally analyzed for determining the extraction mechanisms [29]. The proposed reactive extraction model successfully predicted the loading curve, thus suggesting that model 3 accounts for the main phenomena occurring in the system.

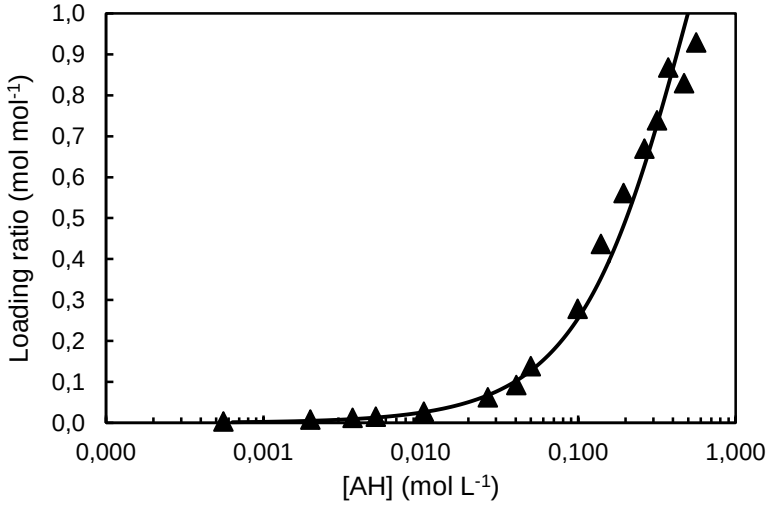


**Figure 8.** Loading curve of 3-HP extraction with DDMA (0.45 mol $L^{-1}$) in 1-dodecanol (40% v/v) and dodecane (40% v/v).
Experimental (symbols), Predicted by model 3 (solid line)

The distribution of the acid species in the organic phase calculated with model 3 presented in Figure 9 is in agreement with experimental results obtained by FT-IR about the relative importance of each complexation mechanism. With model 3, $[\overline{CPX_{11}}]$ is indeed the predominant form of the acid in all the studied concentration range. The concentration of 2:1 complex $[\overline{CPX_{21}}]$ reaches the same order of

magnitude as $[\overline{CPX_{11}}]$ for initial acid concentrations higher than 0.13 mol $L^{-1}$ and becomes almost equal to $[\overline{CPX_{11}}]$ at the highest acid concentration of the studied range. Experimentally, $[\overline{CPX_{21}}]$ was detected from the stretching of the carbonyl group $\nu(\mathrm{C}=\mathrm{O})$ for acid concentrations higher than 0.11 mol $L^{-1}$, thus being in accordance with the behavior depicted by the model.

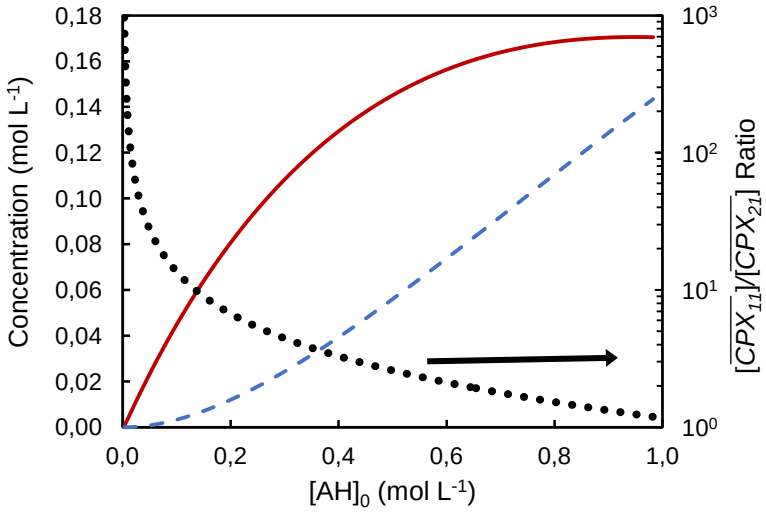


**Figure 9.** Distribution of acid species in the organic phase calculated with model 3, as a function of initial 3-HP concentration
Left y-axis: $[\overline{CPX_{11}}]$ (solid line), $[\overline{CPX_{21}}]$ (dashed line). Right y-axis: $[\overline{CPX_{11}}]/[\overline{CPX_{21}}]$ (dotted line)

Figure 10 presents the graphical estimation of the complexation constants from the experimental data as described in 3.6. The relative abundance of the different complexes could explain the high uncertainty on the graphical estimation of $\mathrm{K}_{21}$ observed in Figure 10b. The condition for yielding a straight line is $[\overline{CPX_{21}}] \gg [\overline{CPX_{11}}]$ and this condition is not fulfilled in the studied range, according to Figure 9.

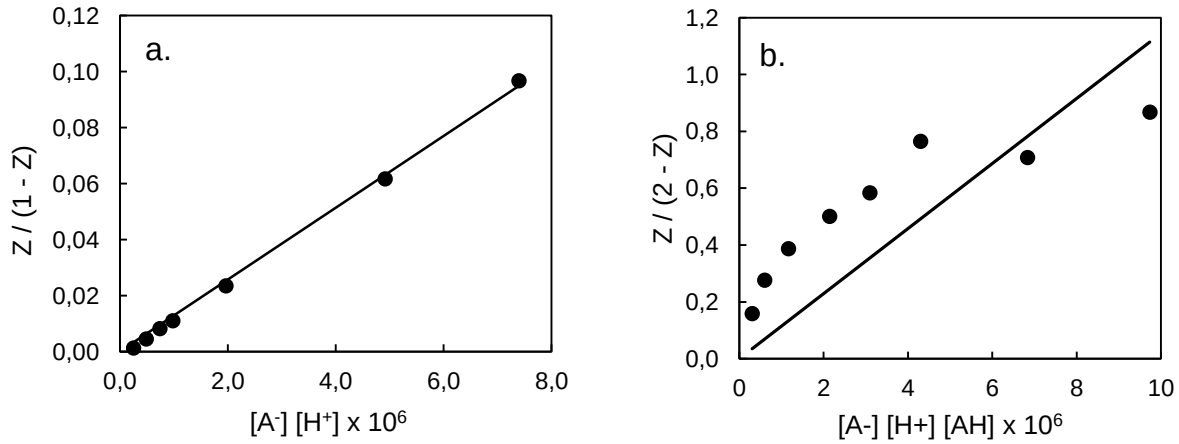


**Figure 10.** Graphical determination of the complexation constants $K_{11}$ and $K_{21}$ a. 1:1 ion-pair complex formation, b. 2:1 hydrogen bonded complex formation. Experimental data (symbols), regression line (solid line).

Despite the high uncertainty, the relative difference of the graphically estimated values (Table 5) remains less than 10% compared to the values in Table 4 obtained by calibration of model 3.

**Table 5.** Graphically estimated complexation constants $K_{11}$ and $K_{21}$

| Parameter | Estimated value | Coefficient of variation [%] |
|---|---|---|
| $K_{11}$ [L$^2$ mol$^{-2}$] | 7.645 | 0.87 |
| $K_{21}$ [L mol$^{-1}$] | 1.49 | 16.4 |

### 5.4. Sensitivity analysis of the model

The goal of global sensitivity analysis is to investigate the changes of model outputs induced by modifications of model parameters. In this work, global sensitivity was evaluated using Sobol indices. Sobol indices, estimated using Monte-Carlo simulations, represent the fraction of the variance of each output that can be explained by variations of each parameter. While decomposing the variance, it is possible to estimate an effect associated to the parameter itself (main effect $S_i$) as well as the interaction between all the parameters. Regarding the interactions, as a matter of simplicity, a total index is defined for each parameter as the sum of its main effect and all the interactions of this parameter with the others ($S_{T_i}$).

The main and total Sobol indices of the parameters were estimated for two model outputs: extraction yield and equilibrium pH. Only main indices are presented in this section as no significant interactions between the parameters were observed. Three main regions can be identified in Figure 11. Region 1 covers initial acid concentrations lower than 0.02 mol $L^{-1}$ and the variance of both outputs is mainly explained by $K_{11}$ and $K_{aq}$. Region 2 covers concentrations in the range 0.02 mol $L^{-1}$ – 0.11 mol $L^{-1}$, where the variance is completely explained by $K_{11}$. Finally, region 3 covers acid concentrations above 0.11 mol $L^{-1}$, where $K_{11}$ and $K_{21}$ are the key parameters explaining the variance.

In region 1, impurities have a moderate effect on extraction yield ($S_{K_{aq}} < 20\%$) but act strongly on the equilibrium pH. Indeed, $K_{aq}$ explains up to 85% of the variance of the equilibrium pH. In this region, the ratio of estimated impurities to the initial acid is equal to 0.71 mol $mol^{-1}$ for the lowest acid concentration and is equal to 0.02 mol $mol^{-1}$ at 0.08 mol $L^{-1}$. At higher acid concentrations, impurities become insignificant compared to acid molecules. The considered side reaction thus significantly contributes to the behavior observed at initial acid concentrations lower than 0.02 mol $L^{-1}$.

In region 2, the whole variance is explained by $K_{11}$. This was expected because $\overline{CPX_{11}}$ is the predominant form of the acid in the organic phase. As $K_{21}$ has no influence on the model outputs in regions 1 and 2, the model could be simplified to 1:1 complex formation plus the side reaction for initial acid concentrations below 0.11 mol $L^{-1}$.

When initial acid concentration exceeds 0.11 mol $L^{-1}$, the effect of $K_{21}$ increases as the initial 3-HP increases (region 3). This behavior is explained referring back to Figure 3 and Figure 9, where it was observed that the 2:1 complex becomes significant at high acid concentrations. In regions 2 and 3 the presence of primary amines can be neglected, and the model could be simplified to 1:1 and 2:1 complex formation without the side reaction (model 2).

a. b.

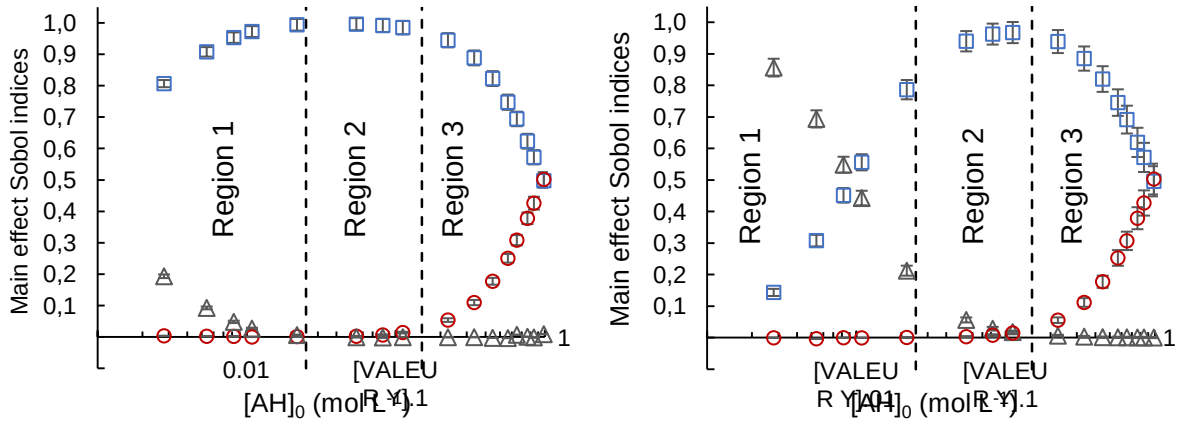


747 **Figure 11**. Sensitivity analysis of the model outputs. a. Extraction yield, b. Equilibrium pH
748 $K_{11}$ (squares), $K_{21}$ (circles), $K_{aq}$ (triangles)
749

750 The sensitivity analysis also explains the observations concerning the uncertainty in
751 parameter estimation (Table 4). The equilibrium constant related to the formation of
752 the 1:1 complex ( $K_{11}$ ) has a high sensitivity for both model outputs in all
753 concentration regions; its estimated value is thus based on the full set of
754 measurements and has the lowest uncertainty (3.2%). The equilibrium constant
755 related to the formation of the 2:1 complex ($K_{21}$) has a good sensitivity for both model
756 outputs but in region 3 only, explaining its higher uncertainty (8.7%). As for the
757 equilibrium constant of the side reaction ($K_{aq}$), its sensitivity is only significant for the
758 pH output in region 1; the number of relevant measurements is thus small and its
759 uncertainty the largest (23.9%).
760
761 Overall, the sensitivity analysis aligns well with the observations of sections 5.1 and
762 5.2 about the contribution of each complexation mechanism and the uncertainty on
763 the parameter estimation (Table 4).
764

765 ## 6. Conclusion
766

767 In this work, we studied the reactive extraction of 3-hydroxypropionic acid with a
768 newly designed biocompatible organic phase consisting in 20% v/v DDMA, 40% v/v
769 1-dodecanol and 40% v/v dodecane. The loaded organic phase, analyzed by FT-IR
770 spectroscopy, allowed to elucidate the reactive extraction mechanism of 3-HP in
771 initial acid concentration range 0.0028 – 1 mol $L^{-1}$. DDMA in these diluents was found
772 to be a stronger base than the dissociated 3-HP ($pK_{a,B} > pK_a$) being capable to bind

a proton from the aqueous phase. A 1:1 stoichiometry complex is then formed from the interaction of the protonated amine and the dissociated acid. Besides, the 1:1 complex is able to extract undissociated acid molecules by the formation of hydrogen bonds leading to the formation of a complex of stoichiometry 2:1. The mathematical model proposed showed that the 1:1 complex predominates in all the studied concentration range. The 2:1 complex becomes significant for initial acid concentrations higher than 0.11 mol $L^{-1}$.

The extraction yield and equilibrium pH prediction were improved by taking into account a side reaction related to the presence of primary amines in the organic phase. The selected model successfully describes two important phenomena observed experimentally at low initial 3-HP concentrations ($< 0.08$ mol $L^{-1}$): poor extraction yield and the underestimation of the predicted pH. The proposed model is thus useful for predicting equilibrium concentrations in the studied range, which corresponds to typical acid concentrations in bioconversion broths

The gained insights into reactive liquid-liquid extraction of organic acids (hereby 3-HP acid), allowed to propose a methodology for mechanistic modeling that can be transposed to the study of reactive liquid-liquid extraction of any particular carboxylic acid of interest.

Equilibrium studies using biocompatible organic phases are essential steps for developing dynamic models of ISPR processes including biological production for bio-based organic acids. The development of such models will contribute to better integrated bioprocess design and optimization.

## 7. Acknowledgements

This work was funded by a doctoral grant awarded from the ABIES doctoral school of Université Paris-Saclay.

## 8. References

[1] C. Mcglade, P. Ekins, The geographical distribution of fossil fuels unused when limiting global warming to 2 °C, Nature. 517 (2015) 187–190. https://doi.org/10.1038/nature14016.

[2] P. Stegmann, M. Londo, M. Junginger, The circular bioeconomy : Its elements and role in European bioeconomy clusters, Resour. Conserv. Recycl. X. 6 (2020) 100029. https://doi.org/10.1016/j.rcrx.2019.100029.

[3] S.K. Panda, L. Sahu, S.K. Behera, R.C. Ray, Research and production of organic acids and industrial potential, Bioprocess. Biomol. Prod. (2019) 195–209. https://doi.org/10.1002/9781119434436.ch9.

[4] S. Kumar, S. Pandey, K.L. Wasewar, N. Ak, H. Uslu, Reactive extraction as an intensifying approach for the recovery of organic acids from aqueous solution: a comprehensive review on experimental and theoretical studies, J. Chem. Eng. Data. 66 (2021) 1557–1573. https://doi.org/10.1021/acs.jced.0c00405.

[5] K.L. Wasewar, Reactive extraction: an intensifying approach for carboxylic acid separation, Int. J. Chem. Eng. Appl. (2012) 249–255. https://doi.org/10.7763/ijcea.2012.v3.195.

[6] A.S. Kertes, C.J. King, Extraction chemistry of fermentation product carboxylic acids, Biotechnol. Bioeng. 28 (1986) 269–282. https://doi.org/10.1002/bit.260280217.

[7] T. Kurzrock, D. Weuster-botz, New reactive extraction systems for separation of bio-succinic acid, Bioprocess Biosyst. Eng. (2011) 779–787. https://doi.org/10.1007/s00449-011-0526-y.

[8] V. Inyang, D. Lokhat, Kinetic studies on propionic and malic acid reactive extraction using trioctylamine in 1-decanol, Chem. Pap. 74 (2020) 3597–3604.

https://doi.org/10.1007/s11696-020-01194-2.

[9] T. Werpy, G. Petersen, Top value added chemicals from biomass Volume I — Results of screening for potential candidates from sugars and synthesis gas top value added chemicals from biomass, United States, 2004. https://doi.org/10.2172/15008859.

[10] J.J. Bozell, G.R. Petersen, Cutting-edge research for a greener sustainable future Technology development for the production of biobased products from biorefinery carbohydrates — the US Department of Energy ' s " Top 10 " revisited, Green Chem. 12 (2010). https://doi.org/10.1039/B922014C.

[11] C. Jers, A. Kalantari, A. Garg, I. Mijakovic, Production of 3-hydroxypropanoic acid from glycerol by metabolically engineered bacteria, Front. Bioeng. Biotechnol. 7 (2019) 1–15. https://doi.org/10.3389/fbioe.2019.00124.

[12] F. de Fouchécour, A.K. Sánchez-Castañeda, C. Saulou-Bérion, H.É. Spinnler, Process engineering for microbial production of 3-hydroxypropionic acid, Biotechnol. Adv. 36 (2018) 1207–1222. https://doi.org/10.1016/j.biotechadv.2018.03.020.

[13] S.S. Bhagwat, Y. Li, Y.R. Cortés-Peña, E.C. Brace, T.A. Martin, H. Zhao, J.S. Guest, Sustainable production of acrylic Acid via 3-hydroxypropionic acid from lignocellulosic biomass, ACS Sustain. Chem. Eng. 9 (2021) 16659–16669. https://doi.org/10.1021/acssuschemeng.1c05441.

[14] F. Chemarin, M. Moussa, F. Allais, I.C. Trelea, V. Athès, Recovery of 3-hydroxypropionic acid from organic phases after reactive extraction with amines in an alcohol-type solvent, Sep. Purif. Technol. 219 (2019) 260–267. https://doi.org/10.1016/j.seppur.2019.02.026.

[15] A.K. Sánchez-Castañeda, M. Moussa, L. Ngansop, I.C. Trelea, V. Athès,

Organic phase screening for in-stream reactive extraction of bio-based 3-hydroxypropionic acid: biocompatibility and extraction performances, J. Chem. Technol. Biotechnol. 95 (2019) 1046–1056. https://doi.org/10.1002/jctb.6284.

[16] A.D. Pérez, V.M. Gómez, S. Rodríguez-Barona, J. Fontalvo, Liquid − liquid equilibrium and molecular toxicity of active and inert diluents of the organic mixture tri-iso-octylamine/dodecanol / dodecane as a potential liquid membrane for lactic acid removal, J. Chem. Eng. Data. 64 (2019) 3028–3035. https://doi.org/10.1021/acs.jced.9b00132.

[17] G. Burgé, M. Moussa, C. Saulou-Bérion, F. Chemarin, M. Kniest, F. Allais, H.E. Spinnler, V. Athès, Towards an extractive bioconversion of 3-hydroxypropionic acid: study of inhibition phenomena, J. Chem. Technol. Biotechnol. 92 (2017) 2425–2432. https://doi.org/10.1002/jctb.5253.

[18] R. Canari, A.M. Eyal, Extraction of carboxylic acids by amine-based extractants: Apparent extractant basicity according to the pH of half-neutralization, Ind. Eng. Chem. Res. 42 (2003) 1285–1292. https://doi.org/10.1021/ie010578x.

[19] R.R. Grinstead, J.C. Davis, Base strengths of amine-amine hydrochloride systems in toluene, J. Phys. Chem. 72 (1968) 1630–1638. https://doi.org/10.1021/j100851a041.

[20] M. Puttemans, L. Dryon, D.L. Massart, Extraction of organic acids by ion-pair formation with tri-n-octylamine. Part 3. Influence of counter-ion and analyte concentration, Anal. Chim. Acta. 165 (1984) 245–256. https://doi.org/10.1016/S0003-2670(00)85206-X.

[21] J.A. Tamada, C.J. King, Extraction of carboxylic acids with amine extractants. 2. chemical interactions and interpretation of data, Ind. Eng. Chem. Res. 29

(1990) 1327–1333. https://doi.org/10.1021/ie00103a036.

[22] D. Datta, S. Kumar, H. Uslu, Status of the reactive extraction as a method of separation, J. Chem. 2015 (2015). https://doi.org/10.1155/2015/853789.

[23] A.R. Katritzky, R.L. Parris, E.S. Ignatchenko, S.M. Allin, M. Siskin, Reaction of aliphatic amines with 49% formic acid . l ) N,N-dimethyl-1-dodecylamine, Engineering. 339 (1997) 59–65. https://doi.org/10.1002/prac.19973390109.

[24] D.R. Lide, ed., CRC Handbook of chemistry and physics (internet version), 96th ed., CRC Press, 2016.

[25] M.J.W. Jansen, Analysis of variance designs for model output, Comput. Phys. Commun. 117 (1999) 35–43. https://doi.org/10.1016/S0010-4655(98)00154-4.

[26] A. Saltelli, P. Annoni, I. Azzini, F. Campolongo, M. Ratto, S. Tarantola, Variance based sensitivity analysis of model output. Design and estimator for the total sensitivity index, Comput. Phys. Commun. 181 (2010) 259–270. https://doi.org/10.1016/j.cpc.2009.09.018.

[27] G. Kaur, K. Elst, Development of reactive extraction systems for itaconic acid: A step towards in situ product recovery for itaconic acid fermentation, RSC Adv. 4 (2014) 45029–45039. https://doi.org/10.1039/c4ra06612j.

[28] F. Chemarin, M. Moussa, M. Chadni, B. Pollet, P. Lieben, F. Allais, I.C. Trelea, V. Athès, New insights in reactive extraction mechanisms of organic acids: An experimental approach for 3-hydroxypropionic acid extraction with tri-n-octylamine, Sep. Purif. Technol. 179 (2017) 523–532. https://doi.org/10.1016/j.seppur.2017.02.018.

[29] J.A. Tamada, A.S. Kertes, C.J. King, Extraction of carboxylic acids with amine extractants. 1. equilibria and law of mass action modeling, Ind. Eng. Chem. Res. 29 (1990) 1319–1326. https://doi.org/10.1021/ie00103a035.

[30] D. Datta, S. Kumar, Reactive extraction of pyridine carboxylic acids with N,N-dioctyloctan-1-amine: experimental and theoretical studies, Sep. Sci. Technol. 48 (2013) 898–908. https://doi.org/10.1080/01496395.2012.712591.

[31] J.J. Max, C. Chapados, Infrared spectroscopy of aqueous carboxylic acids: comparison between different acids and their salts, J. Phys. Chem. A. 108 (2004) 3324–3337. https://doi.org/10.1021/jp036401t.

[32] H. Ziegenfuß, G. Maurer, Distribution of acetic acid between water and organic solutions of tri-n-octylamine, Fluid Phase Equilib. 102 (1994) 211–255. https://doi.org/10.1016/0378-3812(94)87078-0.

[33] W. Qin, Z. Li, Y. Dai, Extraction of monocarboxylic acids with trioctylamine: equilibria and correlation of apparent reactive equilibrium constant, Ind. Eng. Chem. Res. 42 (2003) 6196–6204. https://doi.org/10.1021/ie021049b.

[34] A.M. Eyal, R. Canari, pH dependence of carboxylic and mineral acid Extraction by Amine-Based Extractants: Effects of pKa, Amine Basicity, and Diluent Properties, Ind. Eng. Chem. Res. 34 (1995) 1789–1798. https://doi.org/10.1021/ie00044a030.

[35] F. Chemarin, M. Moussa, F. Allais, V. Athès, I.C. Trelea, Mechanistic modeling and equilibrium prediction of the reactive extraction of organic acids with amines: A comparative study of two complexation-solvation models using 3-hydroxypropionic acid, Sep. Purif. Technol. 189 (2017) 475–487. https://doi.org/10.1016/j.seppur.2017.07.083.

[36] V. Inyang, D. Lokhat, Reactive extraction of malic acid using trioctylamine in 1–decanol: equilibrium studies by response surface methodology using Box Behnken optimization technique, Sci. Rep. 10 (2020) 1–10. https://doi.org/10.1038/s41598-020-59273-z.

[37] V.R. Dhongde, B.S. De, K.L. Wasewar, Experimental study on reactive extraction of malonic acid with validation by Fourier Transform Infrared Spectroscopy, J. Chem. Eng. Data. 64 (2019) 1072–1084. https://doi.org/10.1021/acs.jced.8b00972.

[38] N. Thakre, A.K. Prajapati, S.P. Mahapatra, A. Kumar, A. Khapre, D. Pal, Modeling and optimization of reactive extraction of citric acid, J. Chem. Eng. Data. 61 (2016) 2614–2623. https://doi.org/10.1021/acs.jced.6b00274.

[39] G. V. Gusakova, G.S. Denisov, A.L. Smolyanskii, A spectroscopic study of the interaction of isobutyric acid with pyridine and dioxan, J. Appl. Spectrosc. 14 (1971) 628–632. https://doi.org/10.1007/BF00605803.

[40] G.M. Barrow, The nature of hydrogen bonded ion-pairs: the reaction of pyridine and carboxylic acids in chloroform, J. Am. Chem. Soc. 78 (1956) 5802–5806. https://doi.org/10.1021/ja01603a022.

[41] G. V. Gusakova, G.S. Denisov, A.L. Smolyanskii, Spectroscopic investigation of the reaction of acetic and isobutyric acids with tertiary amines, J. Appl. Spectrosc. 17 (1972) 1321–1325. https://doi.org/10.1007/BF00940374.

[42] J.W. Smith, M.C. Vitoria, Infrared spectroscopic investigations of acid–base interactions in aprotic solvents. Part I. The interaction of tri-n-propylamine and some carboxylic acids, J. Chem. Soc. A. (1968) 2468–2474. https://doi.org/10.1039/J19680002468.

[43] M. Wierzejewska-Hnat, Z. Mielke, H. Ratajczak, Infrared studies of complexes between carboxylic acids and tertiary amines in argon matrices, J. Chem. Soc. Faraday Trans. 2 Mol. Chem. Phys. 76 (1980) 834–843. https://doi.org/10.1039/F29807600834.

[44] J.A. Tamada, C.J. King, Extraction of carboxylic acids with amine Extractants.

3. effect of temperature, water coextraction, and process considerations, Ind. Eng. Chem. Res. 29 (1990) 1333–1338. https://doi.org/10.1021/ie00103a037.

## 9. Appendices

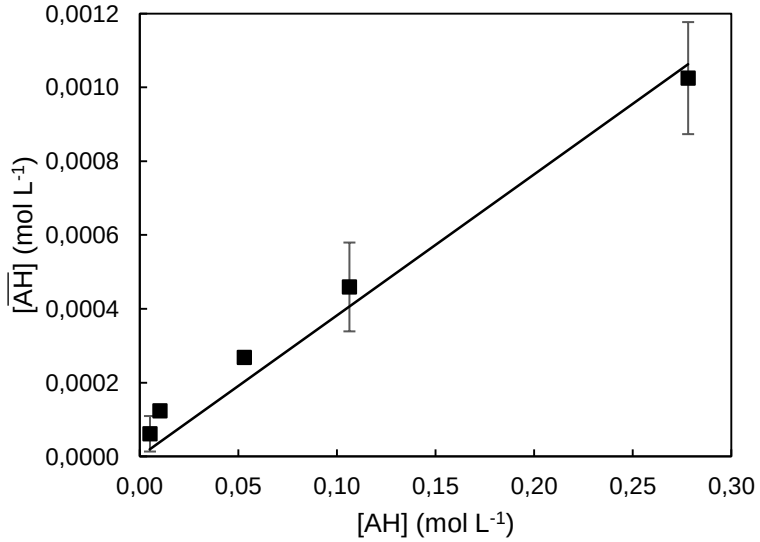


**Figure A1.** Estimation of physical partitioning constant $K_m$. Experimental data (symbols), Regression line (solid line). Error bars correspond to standard deviation ($n = 3$)

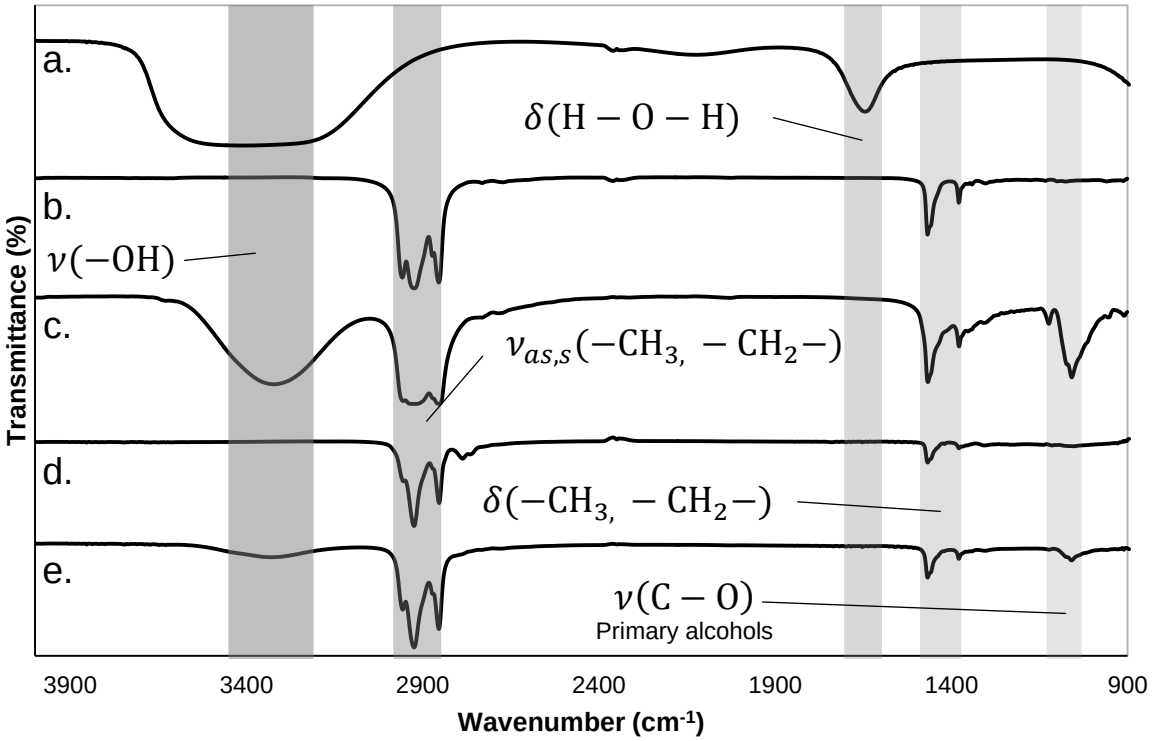


968

969 **Figure A2.** FT-IR spectra of different compounds/phases used in this study
970 a. Water, b. Dodecane, c. 1-dodecanol, c. Purified DDMA, d. Organic phase (40% v/v
971 1-dodecanol, 40% v/v dodecane, 20% v/v purified DDMA)
972